Development of Flow within a Diffusing C-Duct –Experimental Investigation and Numerical Validation

Nirmal K. Das[1], B. Halder[2], P. Ray[3], and B. Majumdar[4]

1(Department of Mechanical Engineering, BCET, Durgapur, West Bengal, India)
2(Department of Mechanical Engineering, NIT Durgapur, West Bengal, India)
3(Department of Civil Engineering, NIT Durgapur, West Bengal, India)
4(Department of Power Engineering, Jadavpur University, Kolkata, West Bengal, India)

ABSTRACT

Experimental investigation of flow development within a rectangular 90º curved diffusing C-duct of low aspect ratio and area ratio of 2 was carried out and the three-dimensional computational results are then compared with the experimental results for numerical validation. All measurements were made in a turbulent flow regime (Re = 2.35×10^5), based on the duct inlet hydraulic diameter (d_h = 0.0666m) and mass averaged inlet velocity of 60m/s. Wall pressures were measured through wall pressure taps. The mean velocities, static and total pressures at six cross-sectional planes (along the centreline of the diffuser) were obtained using a pre-calibrated three-hole pressure probe in null mode. The flow was numerically simulated by using different viscous models available in the commercial CFD software FLUENT 6.3. The experimental inlet and boundary conditions were used as input for the computation and validation of the numerical results.

Based on the comparison, it is found that Standard k–ε turbulence model provides better prediction of flow field in the diffusing C-duct. Numerical results of coefficient of mass averaged static pressure recovery (61.6%) and coefficient of mass averaged total pressure loss (9.1%) are in good agreement with the experimentally obtained static pressure recovery and total pressure loss coefficients of 52.48% and 15.5% respectively.

Keywords - *Aspect ratio, area ratio, coefficient of static pressure recovery, C-shaped diffuser, secondary motion, wall pressure.*

NOMENCLATURE

AR	Area ratio (W_2/W_1)
AS	Aspect ratio (b/W_1)
b	Height of diffuser
cc	Concave
cv	Convex
Cpr	Coefficient of static pressure recovery [$(P_s-P_{savi})/P_{davi}$]
ξ	Coefficient of total pressure loss [$(P_t-P_{tavi})/P_{davi}$]
De	Dean number [$Re/\sqrt{(R_c/d_h)}$]
d_h	Hydraulic diameter[$2 W_1 b/(W_1+b)$]
P_{davi}	Average dynamic pressure at inlet plane ($0.5\rho U_{avi}^2$)
P_s	Average static pressure at a plane
P_{savi}	Average static pressure at inlet plane
R_c	Mean radius of curvature
Re	Reynolds number ($U_{avi} d_h/\nu$)
U_{avi}	Inlet average velocity
w	Width at a measuring section
W_1	Inlet width
W_2	Outlet width
ν	Kinematic viscosity
2θ	Total divergence angle
Δβ	Angle of turn of the centerline

1. INTRODUCTION

In many engineering applications, diffusers are used to convert the dynamic pressure into static pressure. The importance of the diffuser as a single, useful, fluids handling element in wind tunnels, turbo-machinery, and as interconnecting flow passage between the components of gas turbines has been widely known. Understanding of diffuser flows, therefore, is of paramount importance to the design of fluid-flow systems. Diffusers are designed in different shapes and sizes to meet the specific application. Curved diffusers of different centre line shapes find wide uses in the field of aircraft applications to satisfy design compatibility and space restrictions. Flow characteristics in curved diffusers are most complicated due to the influence of centerline curvature, different geometrical parameters like total angle of divergence (2θ), angle of turn (Δβ), area ratio (AR), inlet aspect ratio (AS), centerline shape, etc. as well as the dynamical parameters like inlet Reynolds number, inlet turbulence, etc.

In curved channels the radial pressure gradient, resulting from the centrifugal force acting on the fluid due to the centerline curvature, can produce significant secondary flows. In addition, the adverse stream wise pressure gradient, resulting from the diverging flow passage of curved diffusers, can lead to flow separation. The combined effect may result in non-uniformity of total pressure and total pressure loss at diffuser exit, thus affecting the diffuser performance.

From the beginning of the last century, study of internal flow through ducts was the area of interest for many researchers. With the advancement of aircraft industry, the flow field characteristics and performance of curved diffusers have been the research topics of interest.

Williams *et al.*, 1902, [1], were the first to investigate flow in curved pipes, where they observed the maximum axial velocity to shift towards the outer wall of the curved pipe. Since then, numerous investigations have been carried out on curved pipes/ducts to establish the effect of various parameters. According to these studies, the secondary flows are generated in the curved pipes either due to the non-uniform distribution of velocity at the inlet and/or due to the effect of centrifugal force.

The complex nature of flow within curved pipes was investigated experimentally by Eustice, 1910, 1911, [2, 3], where he has pointed out the formation of secondary flow as one of the main flow characteristics in curved pipes.

Probably, Fox & Kline, 1962, [4], carried out the first systematic studies of flow regimes on curved diffusers and additional studies of flow regimes in 2-D straight walled diffusers. They developed maps of flow regimes for stalled and unstalled curved diffusers for a range of flow turning angle from 0 to 90º, in steps of 10º, and with curved diffuser geometry having a circular arc centre line and a linear area distribution normal to the centre line.

Bansod and Bradshaw, 1972, [5], made experimental investigation of flow through a number of S-shaped ducts of different geometric parameters, each with a thin inlet turbulent boundary layer. From the measured total pressure, static pressure, surface shear stress and flow yaw angle they have established that the large departure from axisymmetry of flow in the exit plane of the S-duct were due to the expulsion of boundary-layer fluid by a strong longitudinal pair of contra-rotating vortices embedded in the boundary layer.

Sajanikar *et al.*, 1982, [6], studied the effect of turning angle and Reynolds number on the performance of curved diffusers in terms of pressure recovery. Experiments were conducted on fixed area ratio curved diffusers by varying the turn angle between 0° to 90°, in steps of 15° and the Reynolds number between $2x10^4$ to $5x10^5$. From the obtained results they reported that, for a given curved diffuser the pressure recovery decreased with increase in turn angle but increased with increase in Reynolds number.

Computational analysis of fully-developed turbulent flow of an incompressible viscous fluid in curved ducts of square section was reported by Hur and Thangam, 1989, [7]. They used finite volume method in their numerical study with a nonlinear K-*l*

model to represent the turbulence. The results of both straight and curved ducts were presented, where in case of fully-developed turbulent flow in straight ducts the secondary flow was reported by an eight vortex structure. With introduction of moderate curvature authors observed a substantial increase in the strength of secondary flow with a change in the pattern to either a double-vortex or a four-vortex configuration. Their computed results in comparison to available experimental data were reported to be in good agreement. In their opinion the nonlinear K-*l* and K-ε models have the promise to yield more accurate predictions for curved turbulent flows than the more commonly used eddy viscosity models.

By carrying out flow visualisation and wall static pressure measurements on an elliptical centre line 90º curved diffuser of large area ratio (AR = 3.4), Agrawal and Singh, 1991, [8], detected large separation pockets on the convex wall. The separated flow affected the diffuser performance severely and the performance evaluation showed poor pressure recovery and high losses.

Majumdar and Agrawal, 1996, [9], performed an experimental study for air flow in a large area ratio curved diffuser (AR = 3.4, Δβ = 90º, and AS = 0.685) by installing a row of vanes at different angles to the diffuser inlet. Significant development of flow distribution inside diffuser with increased pressure recovery coefficient was achieved when the flow was deflected by 10° towards the convex wall.

In a later study, Majumdar *et al.*, 1998, [10], made detailed experimental investigation of flow in a high aspect ratio (AS = 6) 90° curved diffuser. The observed shift of stream wise bulk flow towards the concave vertical wall was attributed to the centrifugal effect arising out of the centerline curvature. The wall static pressure increased continuously on both the convex and concave walls due to diffusion and a pressure recovery coefficient of 50% was obtained. They also observed that except for a small pocket on the convex wall at the exit there was no flow separation in the diffuser. Counter rotating vortices were detected from 30º turn of the diffuser.

Experimental and numerical studies of turbulent flow in a rectangular curved diffuser (AR = 2, Δβ = 180º, 2θ = 9.12º, and AS = 2) were carried out by Djebedjian, 2001, [11]. The test was carried out at Re = $4.59x10^5$, based on the inlet hydraulic diameter of 0.0666m and mass averaged inlet velocity of 33.7m/s. The maximum velocity core shifted gradually from the convex wall towards the concave wall as the flow moved downstream. The stream-wise velocity along the convex wall was observed to decrease rapidly up to the turn of 90º, approached to zero at 90º and in the downstream theflow was separated with expanding recirculation towards the exit. Wall static pressure recovery along

convex wall was significantly more than that on concave wall and the overall pressure recovery was only 27%. Time-averaged Navier-Stokes equations were used for numerical analysis. The standard k-ε turbulence model and a non-equilibrium k-ε model were tested and evaluated against the experimental data. Both the turbulence models could not predict at par with the experimental results, the separation position and the reattachment length.

Using the commercial CFD code FLUENT, Dey *et al*., 2002, [12], studied numerically the effect of area ratio and turning angle on the performance of circular cross-section S-diffusers. Investigation was done with steady incompressible flow through diffusers, keeping the centre line length and inlet velocity (40m/s) fixed. Computations were made with different values of area ratios of 1.5, 2.0, 2.5, and 3.0 and different turning angles of 15°/15°, 22.5°/22.5°, and 30°/30°. Counter rotating vortices were observed to be present throughout the diffuser length with increasing magnitudes at higher angle of turn. Influence of turning angle on pressure recovery was very less, only 1% fall in static pressure recovery was predicted with the change in turning angle from 15°/15° to 30°/30°. Increase in area ratio registered strong increase in static pressure recovery with reduction in the magnitude of the cross-velocity. They predicted higher number of pairs of vortices to generate for an area ratio of 3.

Sedlář, and Příhoda, 2007, [13], modeled numerically the flow phenomena occurring in turbulent flows through rectangular curved diffusers of AR = 1.5, Δβ = 90°, with straight inlet and exit parts. To find the relationship of the hydraulic losses with the ratio of inner wall radius to the diffuser height (R_i/W_i) and the Dean number (De), investigation was carried out at various inlet Reynolds numbers $(1\times10^5$ to $1\times10^6)$ and different R_i/W_i (1 to 6) keeping the diffuser height constant. Authors used the ANSYS CFX package to solve the three-dimensional Reynolds-averaged Navier-Stokes equation together with different suitable turbulence models. Regions of flow separation were marked and were found to be dependent both on diffuser geometry and Reynolds number. Secondary flows of different structures of multiple vortices were found to form which were influenced mainly by the nature of flow separation.

2. EXPERIMENTAL AND COMPUTATIONAL FACILILITY

The experiments were conducted in the Aerodynamics Laboratory, National Institute of Technology, Durgapur, India. The measurements were carried out in an open-circuit wind tunnel (Fig.1). The rate of mass flow of air through the test rig was controlled by throttling the blower suction with the help of a flap gate mounted on it. The 90°curved diffuser was designed with circular arc centre line, as suggested by Fox and Kline [4]. The

rectangular cross-section was increased in area by linearly varying the width from 0.05m at inlet to 0.1m at the exit, over the total centre line length of 0.6m while the height was kept constant at 0.1m. The curved part of the test diffuser was fabricated in four segments each of 0.382m centre line radius and subtending an angle of 22.5° at the centre of curvature. Two constant area straight ducts, one preceded while the other succeeded the curved part of the diffuser. The test diffuser was fabricated from transparent acrylic sheets. One hundred eighty evenly distributed wall pressure taps were provided (at six measuring sections as elaborated later) for measurement of wall pressures on the four walls. The mean velocities, static and total pressures at six cross-sectional planes, namely Inlet, A, B, C, D, and Outlet were obtained using a pre-calibrated three-hole pressure probe in null mode. The geometry of the curved diffuser along with the measuring sections is shown in Fig.2.

The geometry of the diffusing C-duct was developed in GAMBIT and subsequently it was meshed with the solver FLUENT 5/6. Flow through the diffuser was numerically simulated by using different viscous models available in the commercial CFD software FLUENT 6.3. The experimental inlet and boundary conditions were used as input for the validation of the viscous models. The 2-D presentations of the computed wall pressure distribution and mean velocity contours were developed by using the graphics software Tecplot'10.

3. RESULT AND DISCUSSION

The flow development in the diffusing C-duct was investigated through measurements of the wall pressure distribution, velocity distribution, pressure distribution and pressure recovery. However, due to the space restriction, the important parameters like the wall pressure distribution, mean velocity distribution, and the pressure recovery are presented here. For validation of different viscous models available in the commercial CFD software 'FLUENT 6.3', the computed results were compared with the experimental results.

3.1 WALL PRESSURE DISTRIBUTION

The measured static pressures on the respective walls were normalized by inlet dynamic pressure and using the software 'Surfer', 2-D isobars were plotted as shown in Fig.3. Fig. 3(a) and (b), referring to top and bottom walls respectively, show the existence of higher pressure along the concave edge with respect to lower pressure along the convex edge at any angle of turn. It reveals that the fluid movement has taken place from concave edge towards the convex side. The pressure distribution on the convex wall at any section up to the 45° turn (Fig.3(c)), shows lower pressure at the centre and higher towards the top andbottom which

signifies a movement of fluid towards the centre from top and bottom. A reverse trend is observed on the concave wall, (Fig.3 (d)). These directions of fluid movement across the flow passage indicate a probable generation of secondary motion in the form of two contra-rotating vortices at least up to 45º turn. The wall pressure distribution on the four walls clearly exhibits a continuous rise in static pressure along the primary direction of flow, as expected in case of a diffuser.

3.2 MEAN VELOCITY DISTRIBUTION

The normalised (by the inlet average velocity) velocity profiles at the six measuring sections are presented in Figs. 4 (a)–(f). The flow at the diffuser entry (Fig. 4(a)) is almost uniform and symmetric except in the vicinity of the top and bottom parallel walls, which appeared to be due to accumulation of low momentum fluid over the walls and the corner effect. Refer Fig. 4(b) for Section-A (angle of turn 11.25º), the flow is seen to accelerate on the convex wall side to balance the relatively slower flow on the other i.e. concave wall. This is due to the higher pressure on the concave wall compared to the convex wall, as a result of strong centrifugal force. At Section-B (angle of turn 33.75º), referring to Fig. 4(c), non-uniformity in the velocity profile at station-5 near the convex wall is observed. This can be attributed to the migration of low momentum fluid to the convex wall due to generated secondary flow. Similar fluid movement was seen from the wall pressure distribution. At Section-C (angle of turn 56.25º), referring to Fig. 4(d), the non-uniformity in the velocity profiles is seen to spread over more area on the convex wall side (station-6 and 7) as compared to the previous section. It indicates migration of more low momentum fluid along the top and bottom walls towards the convex wall. This may be attributed to the combined effect of secondary flow and greater adverse pressure gradient on the convex wall. As the flow moves further down stream, at Section-D (angle of turn 78.75º), greater area on the convex wall side (up to station 5) is infected with low momentum fluid, as seen from the velocity profiles in Fig. 4(e), which may be attributed to the strong adverse pressure gradient on this wall. About the mid horizontal plane, between station-7 and the convex wall, the flow velocity may have been reduced to zero or even the flow may have reversed, giving rise to flow separation on the convex wall over a small area. Due to reduction in velocity, as expected due to gradual expansion of flow passage the centrifugal force on the concave wall is significantly reduced and fluid with higher velocity moves along this wall. Though the non-uniformity in velocity profiles near the convex wall still persists at the Outlet Section (Fig. 4(f)) like that in the previous section, the waviness is reduced to some extent indicating a significant improvement in quality of flow (regarding uniformity). This may be attributed to the effect of flow through straight duct in this part. The overall reduction in flow velocity reaches its peak value at this section. The general pattern of flow is seen to be symmetrical about the mid horizontal plane.

3.3 MEAN VELOCITY CONTOURS

To obtain more detailed information of flow development inside the diffuser, the normalised (by the inlet average velocity) velocity contours in the form of 2-D presentation (Figs. 5(a)-(f)) have been drawn by using the graphics software package SURFER. Fig. 5(a) referring to the Inlet Section, depicts uniform flow throughout the entire cross-section except at some portion close to the top and bottom corners. A similar observation was made from the velocity profiles also. At Section-A, from Fig. 5(b), the flow is seen to accelerate on the convex wall side and move with maximum velocity occupying major portion of the flow cross-section adjacent to the convex wall while the flow on the concave wall is retarded. Similar differences in velocities on the opposite curved walls were also detected from the velocity profiles, the cause of which was discussed in details in the previous article. The velocity contours in Fig. 5(c) clearly depict that low momentum fluid has accumulated on the convex wall and the bulk flow with maximum velocity is pushed towards the opposite wall. Migration of this low momentum fluid affects the uniformity of flow along the convex wall which corroborates the earlier observation of the non-uniformity in the velocity profile near the convex wall (station 5) at Section-B. The bulk flow with maximum velocity still occupies the area between the mid vertical plane and the convex wall. The developed flow at this section is symmetric about the mid horizontal plane. In further down stream at Section-C, refer Fig. 5(d), more and more low momentum fluid is seen to accumulate along the convex wall which affects the uniformity of flow over the wall. Similar trend was observed in the waviness of the velocity profiles at station 6 and 7 on the convex wall side, as discussed in the previous article. Bulk flow with maximum velocity is seen to shift further towards the concave wall, compared to that at the previous section. Flow on the convex wall is retarded more compared to that on the opposite wall; however, stagnation or reversed flow on any part of the convex wall is not observed. At Section-D, Compared to the previous section, more area (about 40% of the total area) near the convex wall is occupied by low momentum fluid and affects the uniformity of flow over there. Similar non-uniformity was reflected through the velocity profiles, spread over large area between station 5 and the convex wall. Bulk flow with maximum velocity is further pushed towards the concave wall, and located almost centrally about the mid vertical

plane. Velocity gradient at the mid horizontal plane between the curved walls indicates the possibility offlow stagnation or even reversed flow on a finite (may be small) area on the convex wall as discussed through mean velocity distributionse. At Outlet Section in Fig. 5(f), the velocity contours depict greater area on the convex wall to be affected by low momentum fluid and the core flow with maximum velocity to be further shifted towards the concave wall and aligned between the mid vertical plane and the concave wall. This is due to the inertia of flow; the fluid tries to maintain its upstream flow direction and moves closer to the concave wall. The pattern of the velocity contours indicate a significant improvement in quality of flow (regarding uniformity) compared to that in the previous section and justifies the installation of the straight duct at the exit of flow.

3.4 PRESSURE RECOVERY AND LOSS COEFFICIENT

The variation of normalised (by the inlet dynamic pressures) average static pressure recovery and total pressure loss, based on average static pressures at different sections and the centre line length of the diffuser is presented graphically in the Fig. 6. The static pressure in the direction of flow is observed to increase continually, with maximum growth in between Section A and B. The total pressure loss in the direction of flow is observed to increase, with maximum increase in between Section A and B. The effectiveness of the diffuser, ξ_o, defined as the pressure recovery capacity of the diffuser in comparison with ideal pressure recovery coefficient (75% for the present diffuser) is found to be 70%.

3.5 NUMERICAL VALIDATION

The flow through the present diffusing C-duct was numerically simulated by using different viscous models available in the commercial CFD software FLUENT 6.3. The experimental inlet and boundary conditions were used as input for the computation and validation of the numerical results. Based on the comparison, it is found that Standard k–ε turbulence model provides better prediction of flow development in the present diffusing C-duct. However, a little deviation between the computational and experimental results may be observed on the concave wall side, velocity distributions obtained from computational analysis are in good agreement with the experimental results; both qualitatively and quantitatively. In Fig.7, the normalised velocities obtained from computational analysis and experimental results are presented in contour form for validation. Numerically obtained coefficient of mass averaged static pressure recovery (61.6%) and coefficient of mass averaged total pressure loss (9.1%) are in good agreement with the experimentally obtained static pressure

recovery and total pressure loss coefficients of 52.48% and 15.5 % respectively. For comparison of the computed results with the experimentally obtained pressure recovery(Cpr) and loss (ξ) coefficients, the same are presented in Fig.8 and Fig.9 respectively. These agreements corroborate that the CFD code using Standard k-ε model can predict the flow and performance characteristics reasonably well for similar geometries with same boundary conditions.

4. CONCLUSIONS

Flow development in a 90° curved C-shaped diffuser, of rectangular cross-section, low aspect ratio and area ratio of 2, was experimentally investigated in a turbulent flow regime (Re = 2.35×10^5), based on the duct inlet hydraulic diameter of 0.0666m and mass averaged inlet velocity of 60m/s. The following conclusions may be drawn from the study.

1. Down the stream, the wall static pressure increased continuously on the four walls due to diffusion.
2. The duct curvature induced strong pressure driven secondary motion, evolved into pair of counter-rotating vortices, ultimately conveyed down stream and broke into large pairs (at least two).
3. In the down stream beyond 33.75° turn, the streamwise bulk flow shifted gradually towards the concave wall side under the influence of centrifugal force with a faster diffusion on the convex wall.
4. Strong adverse pressure gradient developed on the convex wall, leading to probable development of flow stagnation or flow reversal on a small pocket on the convex wall near the outlet.
5. The induced secondary flows convected the low momentum fluid of the boundary layers towards the centre of the duct, degrading the quality of flow by disturbing the uniformity of velocity distribution.
6. Coefficient of static pressure recovery of 52.48° and effectiveness of the diffuser compared with an ideal one of 70 percent was achieved.
7. The CFD code using Standard k-ε model can predict the flow and performance characteristics of C-diffusers in reasonable agreement with the experimental flow field for similar geometries and with same boundary conditions.

REFERENCES

[1] G.S. Williams, C.W. Hubbell, and G.H. Fenkell, Experiments at Detroit, Michigan on the Effect of Curvature upon the Flow of Water in Pipes, *Transaction of ASCE, 1902, vol. 47*, pp. 1-196.

[2]   J. Eustice, Flow of Water in Curved Pipes, *Proc. Royal Society London*, 1910, Series A84, pp. 107-118.

[3]   J. Eustice, Experiments of Streamline Motion in Curved Pipes, *Proc. Royal Society London*, 1911, Series A85, pp.119-131.

[4]   R. W. Fox, and S. J. Kline, Flow Regimes in Curved Subsonic Diffusers, *Trans. of ASME, Journal of Basic Engineering, Sept. 1962*, pp. 303-316.

[5]   P. Bansod, and P. Bradshaw, The flow in S-shaped Ducts, *Aeronautical Quarterly, May 1972*, pp. 131-140.

[6]   M. B. Sajanikar, S Kar, and U. S. Powle, Experimental Investigation of Incompressible Flow in Curved Diffusers, *Proc. 11th National Conference of FMFP*, Hyderabad, India, 1982.

[7]   N. Hur, S. Thangam, and C. G. Speziale, Numerical Study of Turbulent Secondary Flows in Curved Ducts, NASA Contractor Report 181830, ICASE Report No. 89-25, 1989.

[8]   D. P Agrawal, and S. N Singh, Flow Characteristics in a Large Area Ratio Curved Diffuser, *Proc. 18th National Conference of FMFP*, Indore, India, December 1991.

[9]   B. Majumdar, and D. P. Agrawal, Flow Characteristics in a Large Area Ratio Curved Diffuser, *Proc. Instn. Mech. Engrrs.*, 1996, vol. 210, pp. 65-75.

[10]   B. Majumdar, R. Mohan, S. N. Singh, and D. P. Agrawal, Experimental Study of Flow in a High Aspect Ratio 90 Deg Curved Diffuser, *Trans. of ASME, Journal of Fluids Engineering, 1998, vol. 120*, pp. 83-89.

[11]   B. Djebedjian, Numerical and Experimental Investigations of Turbulent Flow in 180º Curved Diffuser, *Proc. FEDSM, ASME Fluids Engineering Division Summer Meeting*, May 29-June 1, 2001, New Orleans, Louisiana, pp. 1-9.

[12]   R. K. Dey, S. Bhavani, S. N. Singh, and V. Seshadri, Flow Analysis in S-shaped Diffusers with Circular Cross-section, *The Arabian Journal of Science and Engineering, 2002, vol. 27*, No. 2C, pp. 197-206.

[13]   M. Sedlář, and J. Příhoda, Investigation of Flow Phenomena in Curved Channels of Rectangular Cross-section, *Journal of Engineering Mechanics, 2007, vol. 14*, No. 6, pp. 387-397.
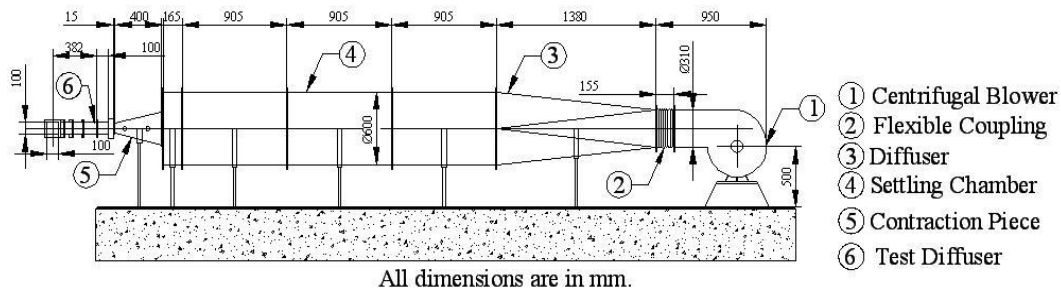
Fig.1 Schematic Diagram of Wind Tunnel with Test Diffuser
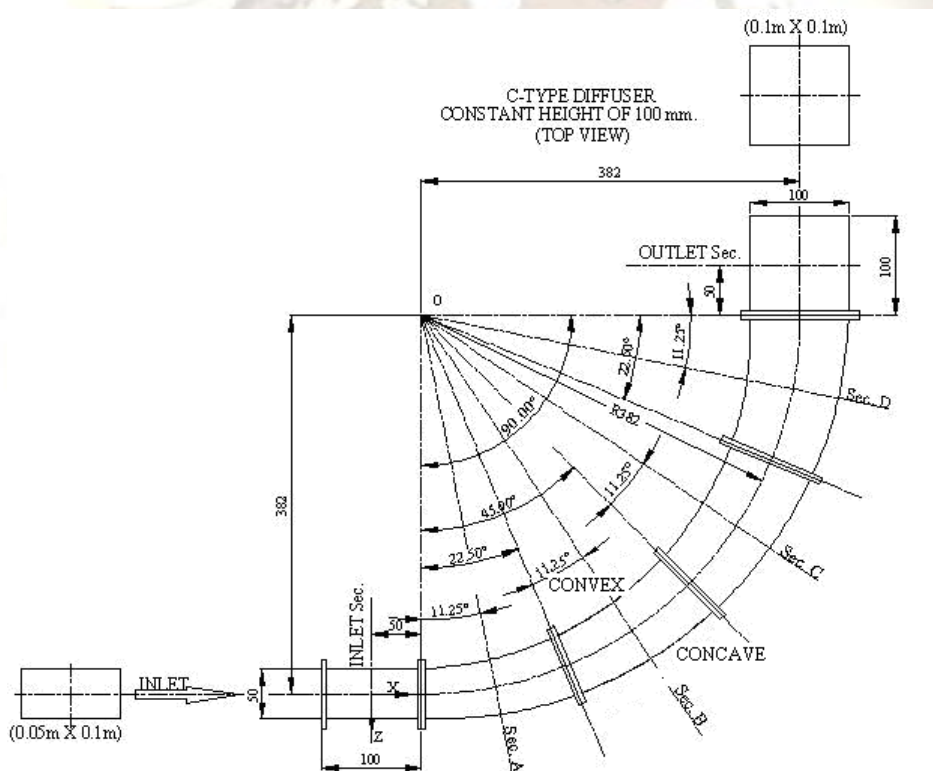
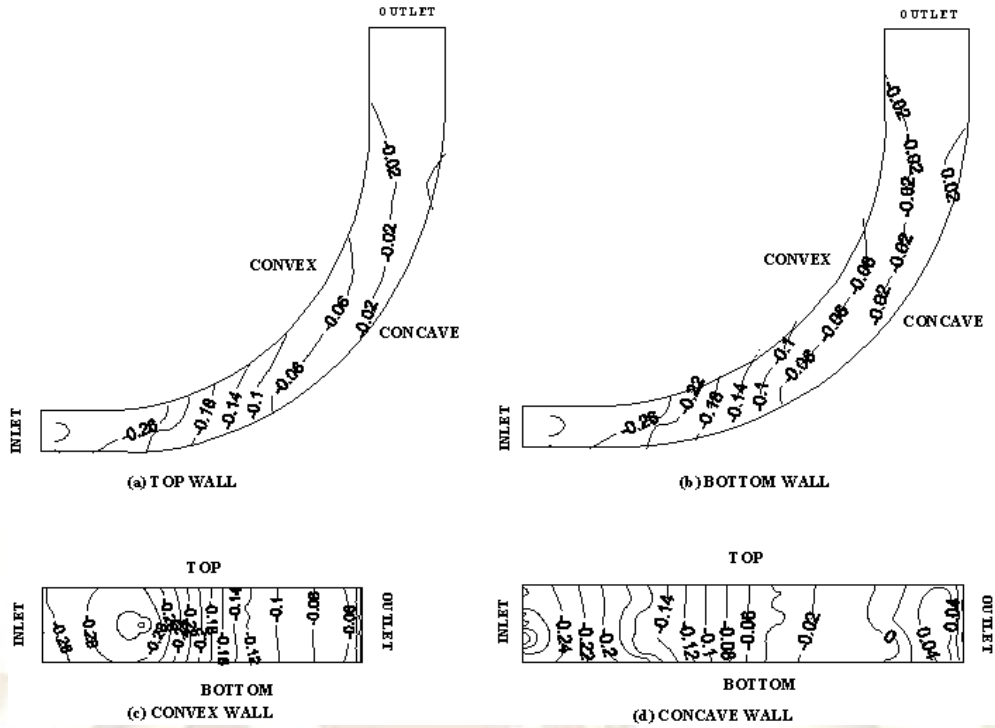**Fig.2 Geometry of Test Diffuser and Measuring sections**
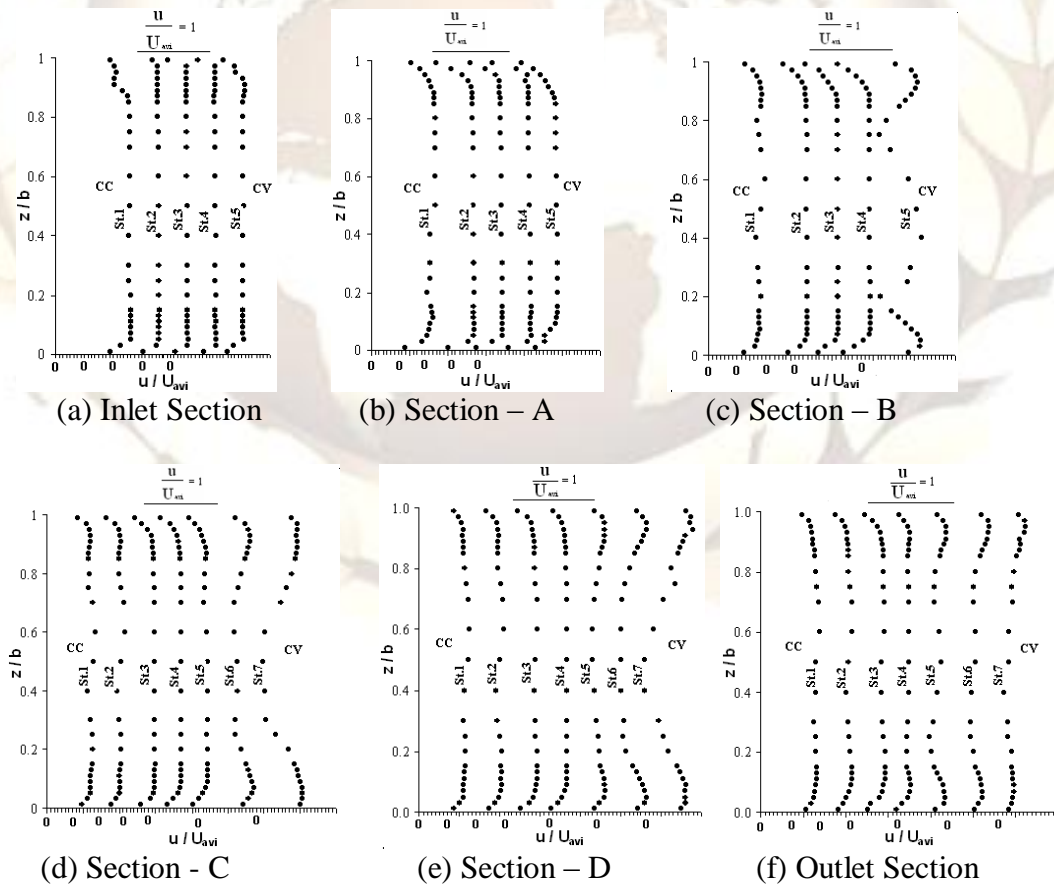
Fig.3 Normalised Wall Pressure Distribution

(a) Inlet Section   (b) Section – A   (c) Section – B

(d) Section - C   (e) Section – D   (f) Outlet Section

Fig.4 Normalised Mean Velocity Profile in Vertical Plane

(a) Inlet Section   (b) Section – A   (c) Section – B

(d) Section – C   (e) Section - D   (f) Outlet Section
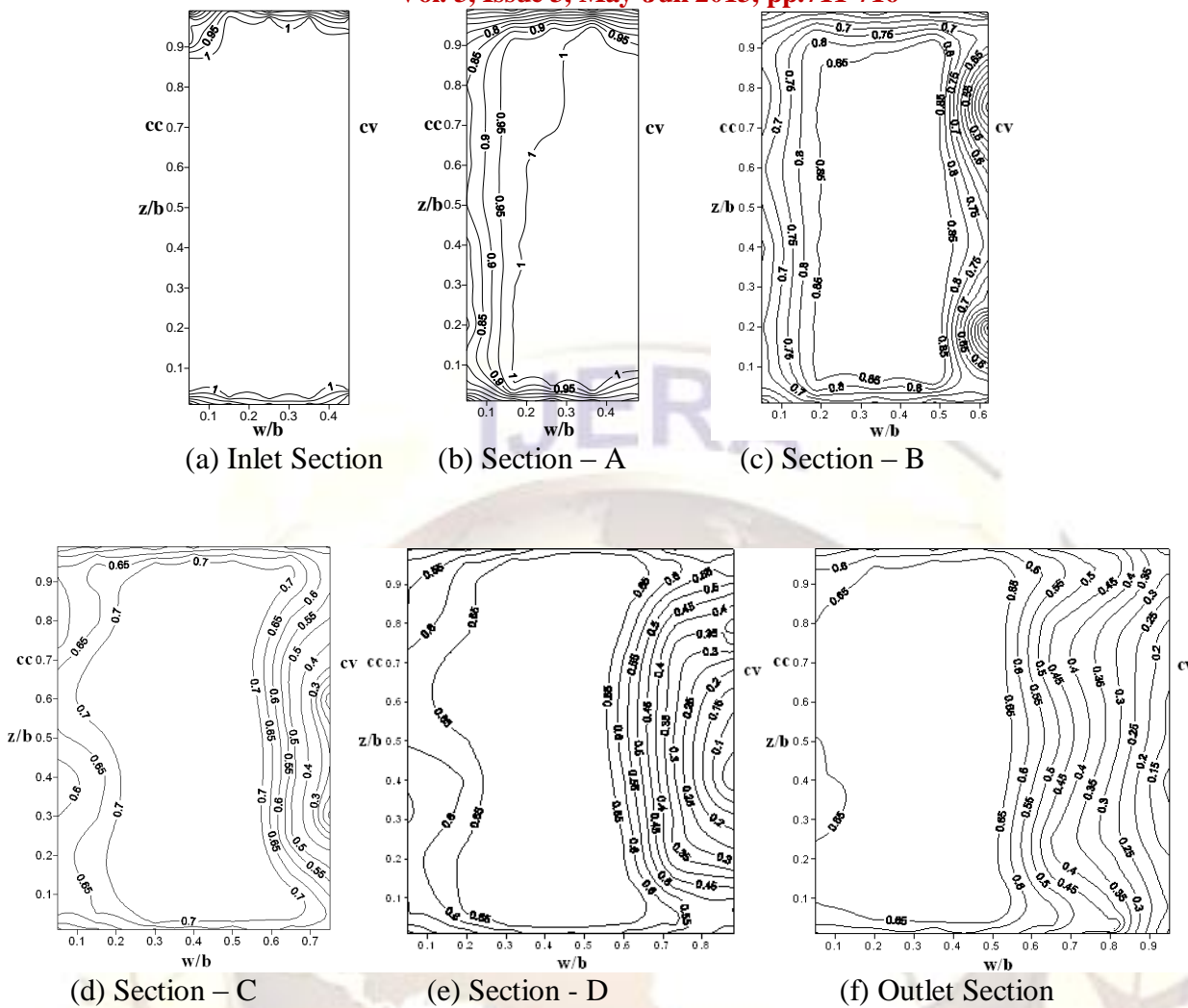
Fig.5 Normalised Mean Velocity Contours
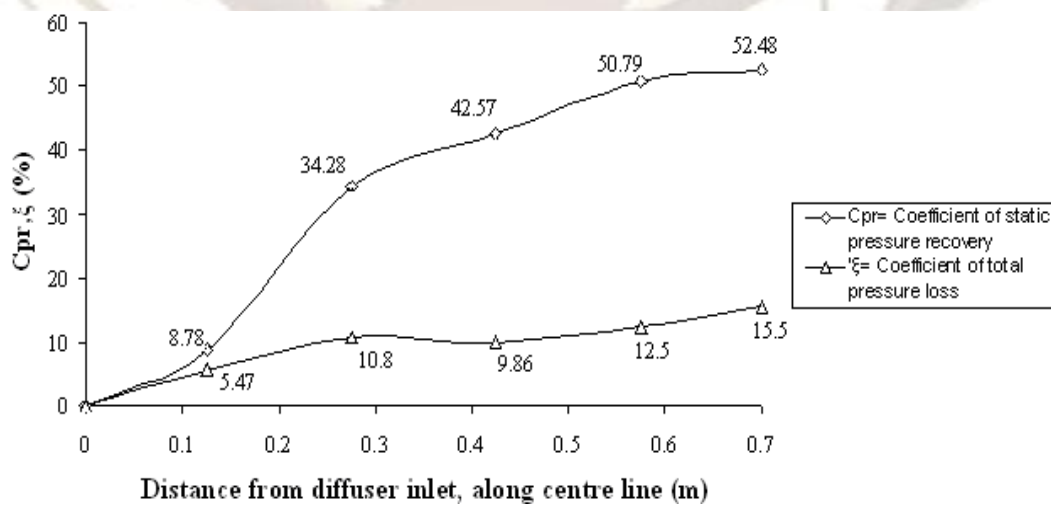
Fig.6 Coefficient of Static Pressure Recovery and Total Pressure Loss
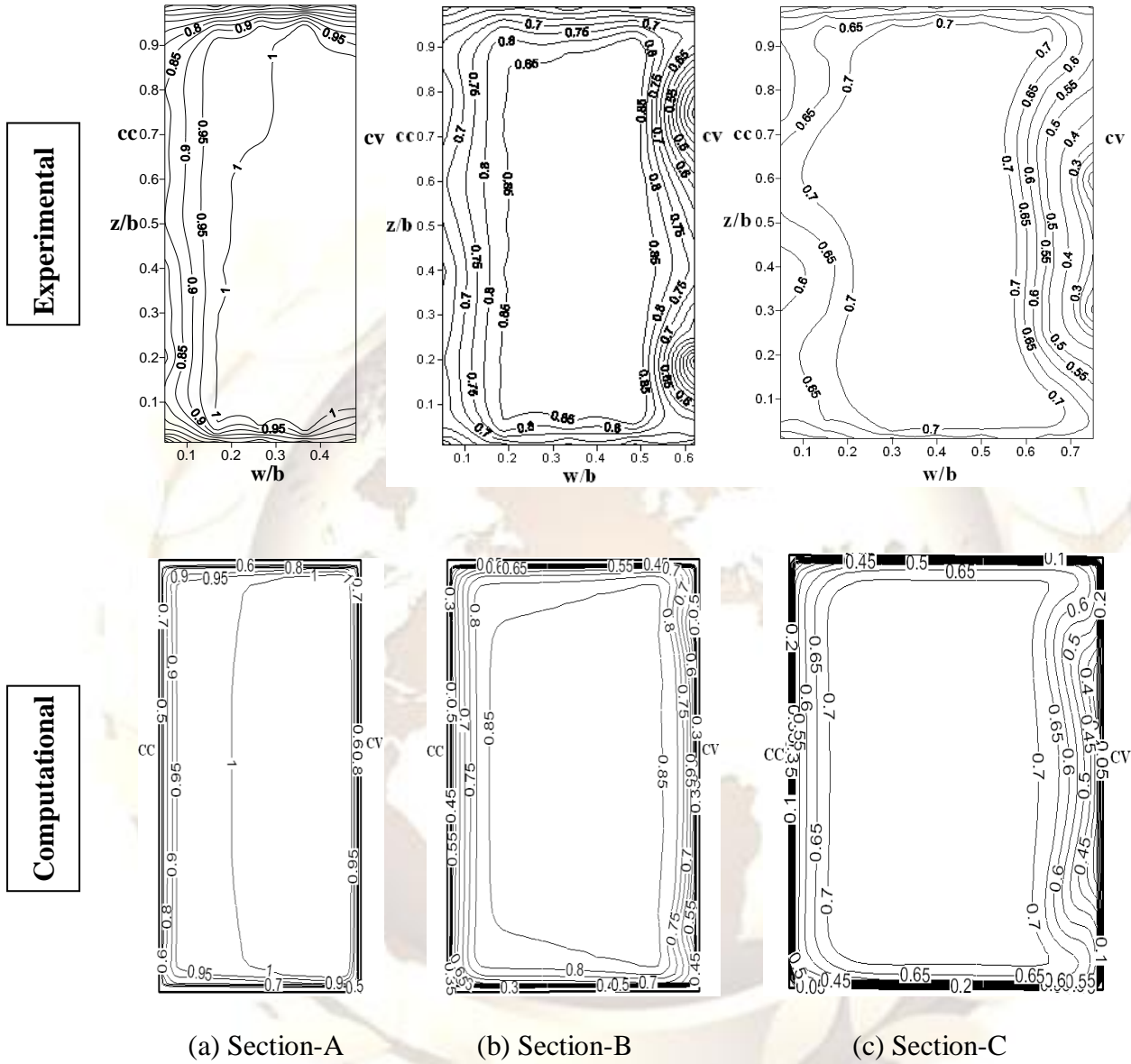
(a) Section-A   (b) Section-B   (c) Section-C

Fig.7 Comparison of Experimental and Computational Normalised Velocity Contours (Contd.)

(d) Section-D   (e) Outlet Section
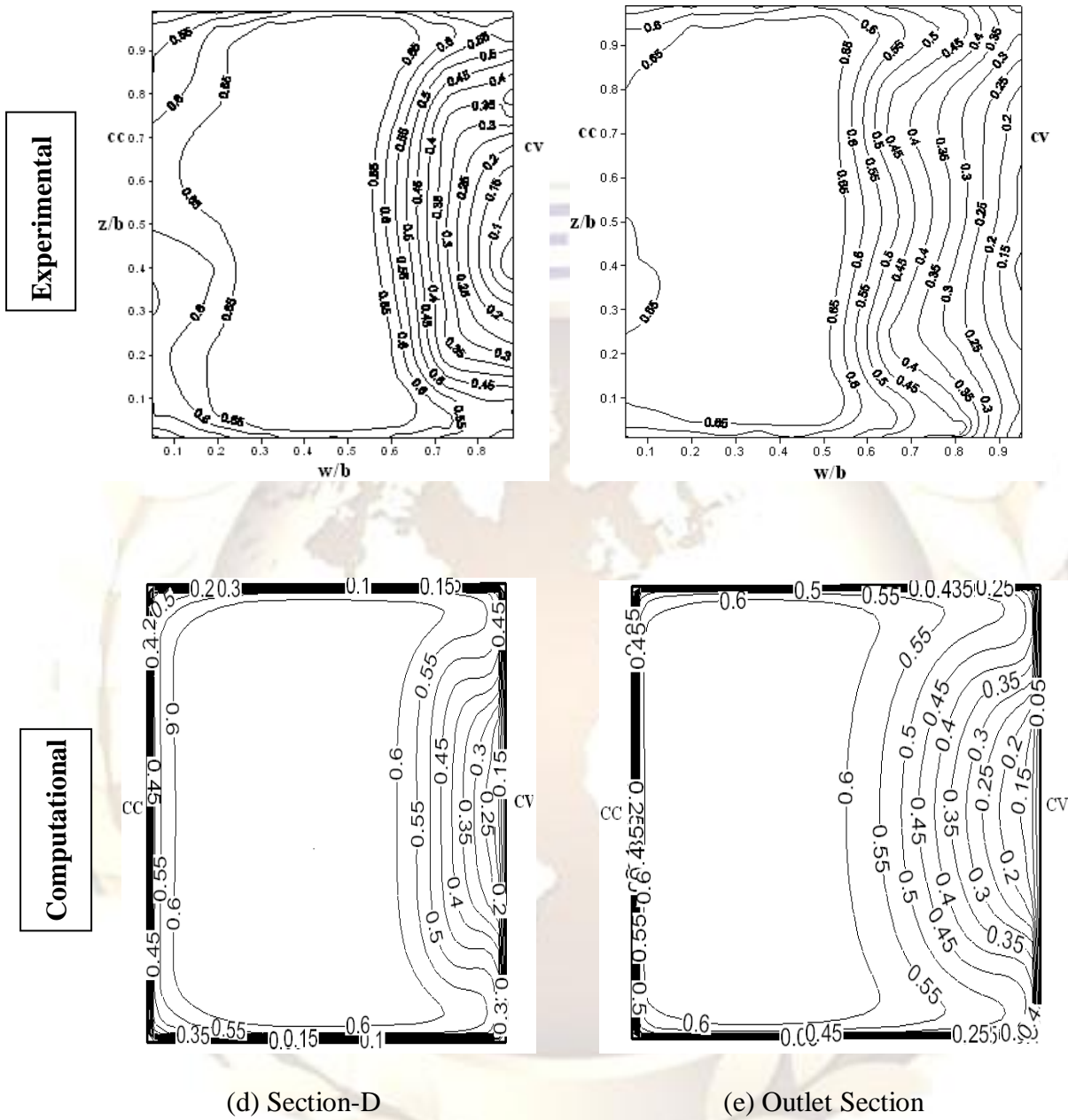
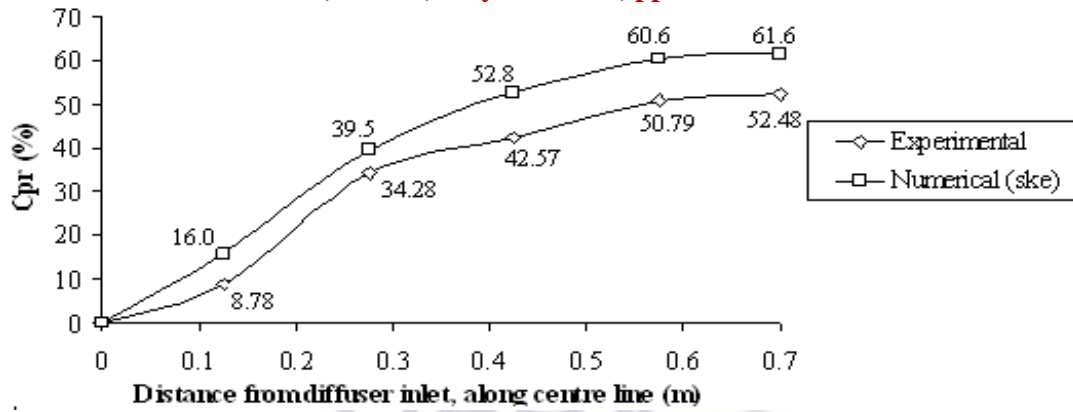**Fig.7 Comparison of Experimental and Computational Normalised Velocity Contours**

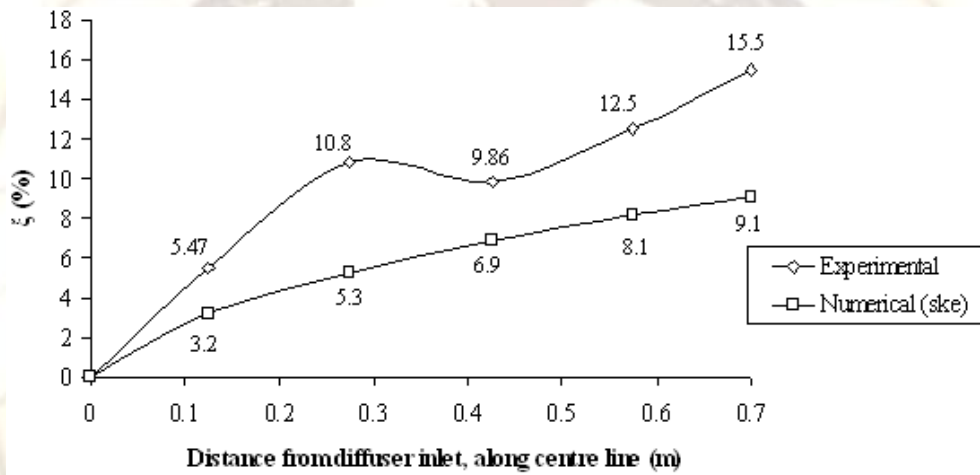**Fig.8 Comparison of Experimental and Computational Pressure Recovery**

Fig.9 Comparison of Experimental and Computational Pressure Loss